

Image Reconstruction of an Electrical Capacitance Tomography System Using an Artificial Neural Network

T. D. Sun^{a,c}, R. Mudde^b, J.C. Schouten^a, B. Scarlett^a, C.M. van den Bleek^a

^aDepartment of Chemical Engineering, Delft University of Technology, The Netherlands

^bDepartment of Transport Phenomena, Delft University of Technology, The Netherlands

^cResearch Institute of Petroleum Processing, Beijing 100083, China

Abstract – In this paper, an image reconstruction algorithm for an electrical capacitance tomography (ECT) system is presented. It is based on an artificial neural network (ANN) Four kinds of grid in the same pipe and with different resolutions are discussed. The sensitivity of a pixel in each grid has been calculated and analyzed. The trained neural network has been applied to experimental data for image reconstruction. Through the cases investigated, a practical image reconstruction strategy for a fluidized bed is suggested.

Key words: ANN, ECT, Image Reconstruction, Fluidized Bed.

1. INTRODUCTION

Electrical Capacitance Tomography (ECT) was developed in the late 1980's as a new kind of technique to measure the spatial distribution of a non-conductive two-phase flow [1][2]. The technique has been developed rapidly during the past 10 years. Some applications of this technique have been reported, such as liquid/gas pipe flow, oil/water/gas gravity separation, pneumatic conveying fluidized beds and flame combustion[5][12][13].

In an ECT system, image reconstruction is a key issue for its application. The most commonly used reconstruction algorithm for an ECT system is the Linear Back Projection (LBP) [3] originally developed for Medical Tomography (MT) systems. The LBP algorithm is very fast, but not very accurate due to the smoothing effects. This algorithm has subsequently been improved for use in a capacitance tomography system[6][6].

Iterative methods, such as least square methods, including direct least squares, damped least squares, weighted least squares and constrained least squares, have been investigated for image reconstruction. It was shown that the constrained least squares method gives the best result[10].

However, image reconstruction results using these methods are far from satisfactory. This is due to the limited number of independent measurements (typically less than 100) in an ECT system and also due to the soft field error. To improve the quality of the image, artificial neural networks were introduced to carry out image reconstruction of ECT data for the first time in 1994. A 12-electrode ECT system was used to recognize pipe flow patterns, such as

bubble flow, core flow, annular flow and stratified flow [8][9]. Based on this, a hybrid method of neural network and fuzzy logic has been studied for the ECT problem[14]. Unfortunately, there is still further work to be done before neural networks can be successfully applied. For example, the image quality in the center area of the pipe is still poor and has to be enhanced.

In this paper, a reconstruction method completely based on a neural network has been studied. First a neural network model was setup, and then the sensitivity of one pixel inside the pipe of different grids was analyzed. With the trained neural network, experimental data were used to verify the methods. Furthermore, some case studies were made to investigate the disadvantages and advantages of the method.

2. ECT SYSTEM AND ITS PROBLEMS

In Fig. 1, the cross-section of a 12-electrode capacitance ECT system is shown.

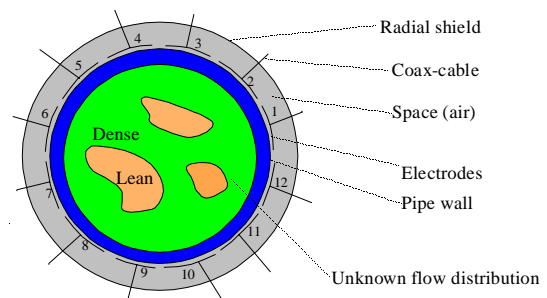


Fig. 1. Cross section of a 12-electrode ECT system

With one of the 12 electrodes of the ECT system charged, and the other 11 electrodes earthed, the capacitance between source electrode (charged) and detector electrode (grounded) was measured. The position of the source electrode changed in from 1 to 12 successively.

2. 1 Solution to the Forward Problem

In terms of Electrical Capacitance Tomography (ECT), the *forward problem* is the problem of calculating the capacitance matrix **C** from a given set of sensor design parameters and a given cross-sectional permittivity distribution ϵ .

$$\epsilon \rightarrow \mathbf{C}$$

The forward model proposed for ECT[3] is based on finite element simulations. It is assumed that both the flow distribution and the electrical field during the measurement set are 2-dimensional and static. Changes in axial direction are neglected within the axial electrode length. Furthermore free charges in the flow are also neglected. Thus, the system obeys the following Poisson equation (2-1):

$$\nabla \cdot [\epsilon(x, y) \nabla \phi(x, y)] = 0 \tag{2-1}$$

Here ϵ is the permittivity distribution, and ϕ is the potential at any position. To calculate the capacitance, the following formulas are used:

$$C_{ij} = Q_{ij} / U_{ij} \tag{2-2}$$

$$Q_{ij} = -\oint_{\Gamma_j} \epsilon(x, y) \nabla \phi(x, y) \cdot \hat{n} dl * H \tag{2-3}$$

Γ_j is a closed curve enclosing the detector electrodes, and H, the electrode length in axial direction. \mathbf{n} is the unit vector normal to Γ_j , Q_{ij} is the induced charge at electrode j when electrode i is the source electrode. The C_{ij} is the capacitance operator between electrodes i and j; U_{ij} is the voltage between the source electrode i and the detector electrode j.

2.2 Image reconstruction

The *inverse problem* of ECT can be formulated as follows: given the electrode potentials applied to the domain boundary as input, and a set of measured capacitances values **C** as output, the permittivity distribution ϵ must be determined. It belongs to the class of parameter estimation problems, in which the model parameters have to be determined from given input and output values.

$$\mathbf{C} \rightarrow \epsilon$$

Image reconstruction aims to solve this inverse problem: to determine the distribution of

dielectric constant within the cross-section from a limited number of measurements.

3. ANN MODEL FOR ECT IMAGE RECONSTRUCTION

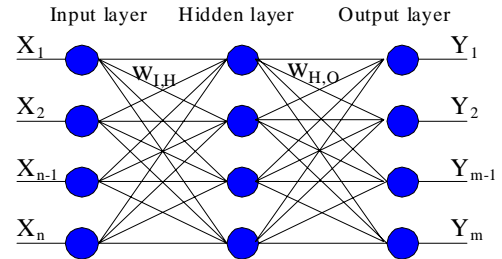


Fig.2 The structure of ANN

Fig. 2 The Structure of ANN

An Artificial Neural Networks (ANN) is shown in Fig 2. There is one input layer, one output layer and one or more layers in the middle (hidden layers). In each layer, there are several nodes or neurons, and a number of connectivities or weights between them. The input to a neuron is either the output from an other neuron or the input vector appropriately weighted by the strength of the connection.

The output response of the j^{th} neuron to an input vector (x_0, x_1, x_n) , is an activation output level (o_j) which is formed by passing a linearly weighted sum of inputs (s_j), through a nonlinear sigmoid function. An extra input (x_0) is defined for the purpose of biasing the neuron. x_0 is always set to unity ($x_0=1$), multiplied by a weight equal to minus the threshold value and added in with all the other inputs. Thus, the output of the neuron is a nonlinear function of the weighted sum of all the inputs (3-1)

$$o_j = f(s_j) \quad \text{where} \quad s_j = \sum_{i=0}^n w_{ij} x_i$$

$$f(s_j) = \frac{1}{1 + e^{-k s_j}} \tag{3-1}$$

Here k is a positive constant that controls the spread of the function.

Such a neural network can be called a 'supervised', one trained with a back-propagation training algorithm for the purpose of pattern classification or pattern association. The training is often more computationally intensive than the forward evaluation of output. The algorithm was developed in 1986[4], and it is called the generalized delta rule or back-propagation rule. This algorithm requires the units to have nonlinear thresholding functions that are continuously differentiable.

A neural network, which consists of one input layer and one output layer without any hidden layers, was employed here to build up the mathematical model.

3.1 Model of the ECT inverse problem.

To set up a neural model for an ECT image reconstruction problem, the internal area of the pipe is divided into many small pixels or neurons, for example 100 neurons (see Fig. 3). The status of one neuron can be described by a value between 0 and 1, meaning empty and fully occupied respectively.

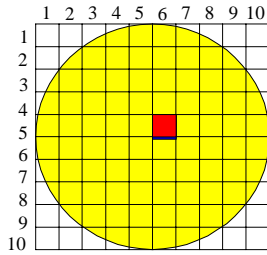


Fig 3.100 neurons

Fig. 3 100 neurons

To determine how many pixels should be used for the model, there are two factors to be considered. One is the system sensitivity of each pixel. The more pixels, the better the image. However, the sensitivity of each pixel will decrease when their size becomes smaller. The other factor is the noise level. When the system is applied to a real process, there is some noise. When the noise level is higher than the sensitivity level, the image results become vague.

There are several possible kinds of grids, in which the pipe is divided into 64, 100, 256, and 400 pixels. For example, a grid of 100 means that the pipe will be divided into 10x10 equal size pixels. In fact, there will only be 88 useful pixels, the other 12 pixels are located outside the pipe and are meaningless.

The input layer of the neural network is a set of capacitance values C , and the output layer is a set of neuron status values.

3.2 Sensitivity analysis

The sensitivity of the pixels in each grid was analyzed. The sensitivity value S is defined as:

$$S = 10 \sqrt{\frac{\sum_{i=1}^n \lambda_i^2}{n}} \quad (0 \leq S \leq 10) \quad (3-2)$$

where,

$$\lambda_i = \frac{C_i - C_{\min}}{C_{\max} - C_{\min}}, \quad (0 \leq \lambda \leq 1) \quad (3-3)$$

n is the independent capacitance number, 66. $i=1, n$. Min. and max. indicate that the lean and dense phase fully occupied the pipe. The results of the sensitivity analysis are shown in Fig.4.

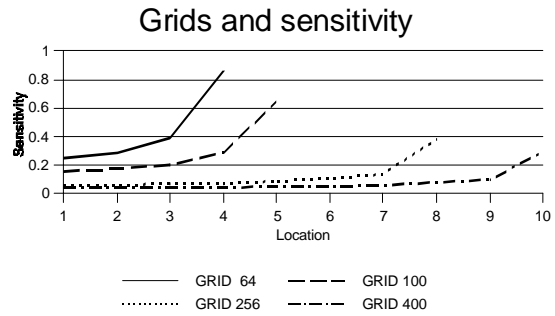


Fig. 4: the sensitivity of a pixel in each grid

In fig. 4, the location 1 to 4 for grid 64 (5, 8, or 10 for grid 100, 256 and 400, respectively) denotes the position from the pipe center to the wall along a radial direction. From fig. 4, the conclusion can be derived that the sensitivity value of a pixel increases from the center of the pipe to the wall. The bigger the size of pixel, the larger the sensitivity value. From fig. 4, it is obvious that the sensitivities in grid 256 and 400 are less than 0.2, but the sensitivities in grid 64 and 100 are larger than 0.2. This can be a critical standard for using the related grids. Comparison between the noise level and the standard value can be made, and suitable grids will be selected.

3.2 Simulation and Training the neural network

As an example, the training process of grid 100 is described. The pipe center is divided in 100 pieces of equal size, and it is assumed that there is only one pixel filled by the dense phase. The capacitances can then be calculated in each case, using a Finite Element Analysis software package SEPRAN, which was developed at TU Delft. As a result, one set of data, which consists of a set of capacitance values and 100 pixels values (full is 1, and empty is 0), i.e. one set of input and output data of the neural network, is obtained. Changing the full pixel position successively, 100 sets of data for training the neural network can be generated.

In our case, there are 66 neurons in the input layer (corresponding to 66 distinct capacitance measurements for a 12-electrode system), 100 neurons in the output layer (corresponding to the spatial image), with no hidden layer connections.

The input vector was normalized to reduce the dynamic range of the capacitance data set. Each neuron in the output layer represents a fragment of the overall image. The function of the neurons in the input layer is purely distributive with no computational overhead, and that of output layer is our target.

For the purpose of training the neural network, the *back-propagation algorithm* was employed. The training procedure is heavily time-consuming.

4. IMAGE RECONSTRUCTION RESULTS

4.1 Experiment # 1: one rod

In this case, a rod was set in a fixed position inside the pipe. The position changed successively from the pipe wall to the center, labeled as P=1 to 5. The pipe diameter was 10 cm. The rod had a diameter of 1.6 cm. In Fig. 5, in the lower line, the rod positions are given. At each position, one set of capacitances was measured.

Using the trained neural network, image reconstruction was carried out with the measured data. In Fig. 5, in the upper line the image reconstruction results are given for a grid of 10*10 pixels. These image results agree with the given positions.

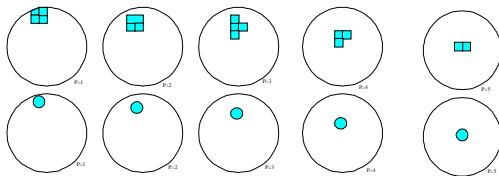


Fig.5 Image reconstruction of ECT: diameter 10cm
P=1,5, represent position from rim to center, the inserted rod diameter is 1.6cm. In the lower line are the original positions. In the upper the image results of grid 100.

4.2 Experiment # 2: two rods

In this case, two rods were set in two fixed positions inside the pipe. The positions changed from the pipe wall to pipe center, labeled as p=1 to 4. The pipe diameter was 10 cm. The rods had a diameter of 1.6 cm. In Fig. 6, in the lower line, the rod positions are given. At each position, one set of capacitances was measured. In the upper line the image reconstruction results are given for a grid of 10*10 pixels. The image results show excellent agreement with the actual positions.

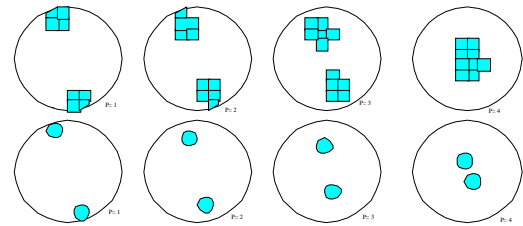


Fig. 6 Image reconstruction of ECT: diameter 10cm
P=1,4, represent position from rim to center
The inserted rod diameter is 1.6cm.
The lower line are setting positions, and
The top line is image reconstruction results of grid 100.

4.3 Image reconstruction results of case 1 and 2 with a grid of 64 pixels

Based on a grid of 64 pixels, the two sets of measured data of case 1 and case 2 were reconstructed, and the results are shown in Fig. 7. The image results show that the agreement with the actual position is good.

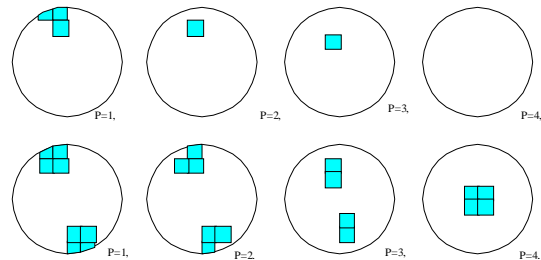


Fig 7 image results of grid 64, the upper line represents the one rod case, The lower line represents the two rods case, P=1,..., 4, represents the location of the rods respectively in accordance with the experimental case 1 and case 2.

4.4 Image reconstruction results of case 1 with grid of 256 pixels

The sets of measured data of experiment #1 were reconstructed, based on a grid of 256 pixels, and the results are shown in Fig. 8. In this case, only in positions p=2, 3,4,5, do the results follow the set points. But when P=1, the image result is poor. The likely explanation for this result is the small gap between the electrodes.

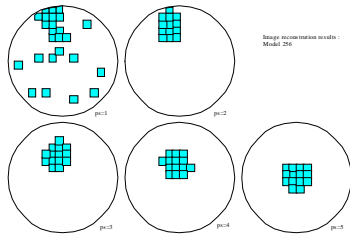


Fig. 8 image results of grid 256 of one rod case, where, $ps=1,5$, represents The location of the rods according to experiments #1.

4.5 Experiments and Analysis: moving objects through the ECT system

4.5.1 experiment #3: moving through center

A cylinder with a diameter of 2.0cm and 3.0cm in height was moved upwards and downwards repeatedly through the pipe center. The moving object was controlled manually, the speed was about 8mm/s.

A series of sensitivity values were derived from the measured data and are shown in Fig. 9. The horizontal axis represents the time ,t, in seconds and the vertical axis represents the signal sensitivity values. In such a case, it shows that the noise level is greater than 0.4 (T =10, 31, 45). The sensitivity analysis was difficult to achieve with all the four grids. Grids of 64 and 100 pixels were applied to carry out the image reconstruction. The peak and valley points were chosen to be treated, and the resulting image results are shown in Fig.10. Generally speaking, the two peaks (T = 20, 39) have been obtained. Unfortunately, unexpected spots also remain where image should be clear (T = 10, 31, 45).

It shows that even in such bad conditions (Sensitivity > 0.4), where the noise level could not be reduced by averaging methods, the neural network can give a general response to the moving object.

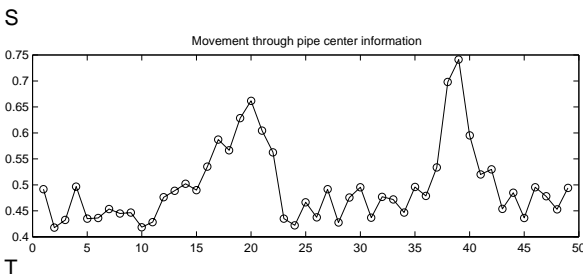


Fig. 9 analysis of object moving through pipe center

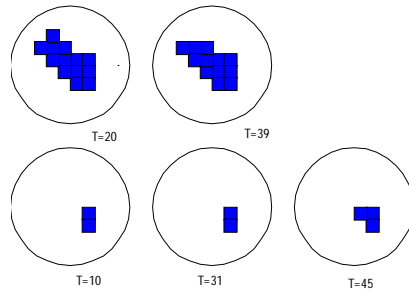


Fig. 10 image results of object moving through pipe center

4.5.2 experiment #4: moving along pipe wall

A cylinder with a diameter of 2.0cm and 3.0cm in height moving upwards and downwards repeatedly near to the pipe wall. A series of sensitivity values derived from the measurement data, are shown in Fig. 11. The horizontal axis represents the time t in seconds and the vertical axis represents the signal sensitivity values. In this case, it shows that the noise level is greater than 0.4 (T= 5, 20, 40), at which moment the object is outside the sensors. Only grids of 64 and 100 pixels can be used to carry out this image reconstruction. The peak and valley points were chosen to be treated, and the resultant image results are shown in Fig.12. The three peaks (T = 13, 33, 47) and the other three valleys (T = 5, 20, 40) have been obtained. Unfortunately, unexpected spots also remain in the center area of the pipe.

It shows that even in such bad conditions (Sensitivity > 0.4), on which the noise level could not be reduced by the average methods, the neural network can give a general response to the moving object.

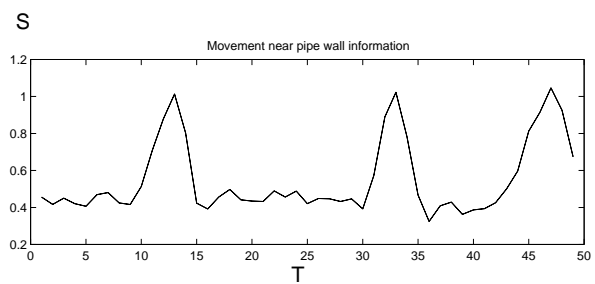


Fig. 11 analysis of object moving near pipe wall

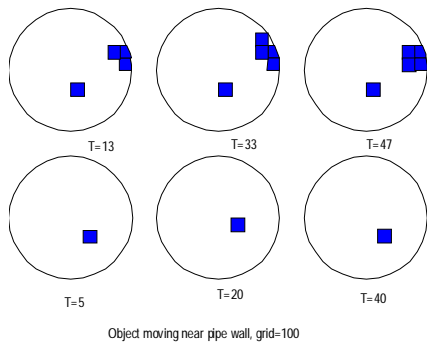


Fig 12. Image results of object moving near pipe wall

4.5.3 comparison of the results in experiment # 3 and # 4, with grid 64

Fig. 9 and Fig. 11 can be combined into one, figure 13, where “o” and “-” lines represents the movement through the pipe center and near to the pipe wall respectively. The same peak and valley points are chosen to be treated. The resultant image results are shown in Fig. 14.

This Figure shows that the results can respond to the movements better than the results with grid 100. Such achievements agree with the conclusions of the sensitivity analysis in paragraph 3.2.

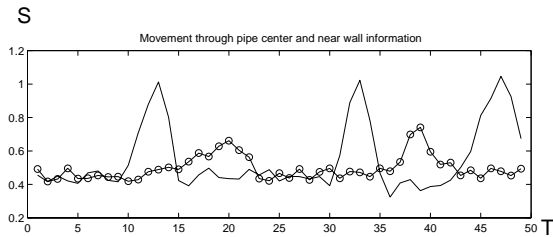
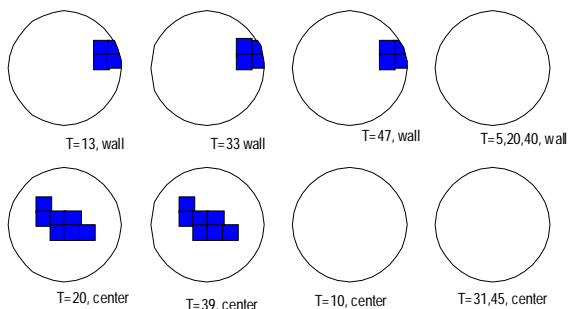


Fig. 13. Analysis of object moving through the pipe center and near wall



Object moving through the pipe center and near pipe wall, grid =64

Fig. 14. Image results of objects moving through pipe center and near pipe wall

5. DISCUSSION

From grid 64 to 256, clear images have been obtained from real measured data and the images agree with the real objects. However, when the objects are located in the pipe center, a poor image results with a grid of 64 pixels. Contrarily, better image results can be obtained when using a grid based on 256 pixels.

The reason for this is that when objects are located in the pipe center, the capacitance signal is weaker than near to the wall, and it is more difficult to reconstruct the measured data. Such results are similar to those of other reconstruction methods, for example the least square methods [Kühn 1997]. Fortunately, such a disadvantage can be overcome by using a neural network with small sized pixels, such as grid 100 and 256.

When two objects meet each other in the center part of the pipe, they are very difficult to distinguish from each other.

The moving objects generated a high noise level in the measurement data, which could not be decreased by averaging. Better image results can be achieved with a lower noise level.

6. CONCLUSION

For this work, the following conclusions can be drawn:

1. An artificial neural network can be used as a method for ECT image reconstruction.
2. Training a neural network is heavily time-consuming.
3. For different levels of noise, different grids should be employed respectively. A sensitivity analysis can be useful in choosing a reasonable grid.
4. In order to overcome the problem of noise, that affects the quality of the image, real data would be better used to train the neural networks.

ACKNOWLEDGEMENTS

The authors are grateful to Mr. ir. J.W.W. Mulder for carrying the experiments, Dr. F.T. Kühn, Mr.ir. R. Bakker and Mr. J. van Raamt are acknowledged for their helpful assistance.

REFERENCES

- [1] Beck, M. S., et. al., "Image for measurements of two phase flow", *Proc. Flow Visualisation IV*, Paris 26-29 August 1986, London Hemisphere, pp. 585-588.
- [2] Huang, S. M., Plaskowski A B, Xie C G, and Beck M S, 1989, "Tomographic imaging of two-flow component flow using capacitance sensor", *J. Phys. E:Sci. Instrum.* 22, pp.173-177.
- [3] Xie, C.G., et. al., "Electrical capacitance tomography for flow imaging: system model for development of image reconstruction algorithms and design of primary sensors", *IEE, Proceedings-G*, vol. 139, No. 1, February 1992, pp. 89-98.
- [4] McClelland, L.& D. Rumelhart, 1991, "Exploration in Parallel Distributed Processing", The MIT Press.
- [5] Isaksen, Ø., "A review of reconstruction techniques for capacitance tomography", *Measurement, Science & Technology* 1996, Vol. 7, No. 3, pp. 325-337.
- [6] Isaksen, Ø. and Nordtvedt, J. E., 1993, "A New Reconstruction Algorithm for Process Tomography", *Measurement, Science & Technology* 1993, Vol. 4, No. 12, pp. 1464-1475.
- [7] Isaksen, Ø. and Nordtvedt, J. E., "An Implicit Model Based Reconstruction Algorithm for use with a Capacitance Tomography System", 1993, *proc. ECAPT*, pp. 144-147.
- [8] Nooralahiyan, A.Y., et. al. , "Neural networks for pattern association in electrical capacitance tomography", *IEEE, proc.-Circuits Devices Syst.*, Vol. 141, No. 6, December 1994, pp. 517-521
- [9] Nooralahiyan, A.Y. ,et. al. , "Performance of neural network with noise and parameter variation in electrical capacitance tomography", *Proc. 4th ECAPT Conf.* Bergen 6-8 April 1995, pp. 420-424.
- [10] Kühn, F.T., et. al., "A least square image reconstruction algorithm for electrical capacitance tomography" , *Frontier in Industrial Process Tomography II*, pp.189-194, April 1997, Delft.
- [11] Kühn, F.T., "Electrical Capacitance Tomography development and application in fluidized bed", Ph.D. Dissertation, 1998, TU Delft.
- [12] Wang, S., et al., "Application of electrical capacitance tomography to flow modeling within circulating fluidized bed", *Frontier in Industrial Process Tomography II*, pp. 33-38, April 1997, Delft.
- [13] Bennett, M.A., et. al., "Electrical Capacitance Tomography applied to pneumatic conveying and flotation processes", *Frontier in Industrial Process Tomography II*, pp. 61-66, April 1997, Delft.
- [14] Peng, L., et al., "The application of artificial neural networks to ECT system", *Frontier in Industrial Process Tomography II*, April 1997, Delft, pp. 287-292.